REPORT DOCUMENTATION PAGE	Form Approved OMB No. 0704-0188

1. AGENCY USE ONLY (Leave blank)	2. REPORT DATE	3. REPORT TYPE AND DATES COVERED
	15 August 95	Final Report 15 AUG 1994 - 15 AUG 1995

4. TITLE AND SUBTITLE

Dynamics of Cracked Composite Material Structures

5. FUNDING NUMBERS

6. AUTHOR(S)

W.M. Ostachowicz, M. Krawczuk, A. Żak

7. PERFORMING ORGANIZATION NAME(S) AND ADDRESS(ES)

Polish Academy of Sciences, Institute of Fluid Flow Machinery
14 Gen. J. Fiszera Street, 80-952 Gdansk, Poland

8. PERFORMING ORGANIZATION REPORT NUMBER

9. SPONSORING/MONITORING AGENCY NAME(S) AND ADDRESS(ES)

U.S. Army Research Office
Edison House, 223 Old Marylebone Rd.
London NW1 5TH, U.K.

10. SPONSORING/MONITORING AGENCY REPORT NUMBER

N68171-94-C-9108

11. SUPPLEMENTARY NOTES

12a. DISTRIBUTION/AVAILABILITY STATEMENT

Approved for public release: distribution unlimited.

12b. DISTRIBUTION CODE

13. ABSTRACT (Maximum 200 words)

As a result of this work models of the finite beam and plate elements have been elaborated, to enable the analysis of the influence of the fatigue cracks and delaminations on the dynamic characteristics of the constructions made of unidirectional composite materials. The method of modelling the crack or delamination presented in the report enables an easy modification of the elaborated elements according to its specific damage (oblique crack, two-side crack, inside crack, multiple delaminations, etc.).

The results of numerical calculations obtained from the crack model are in consistence with the known influence of the position and depth of the crack on the decrease of the natural bending frequencies of the cantilever beam. Simultaneously, a strong influence of the material parameters on these changes has been observed, which does not exist in the case of isotropic materials.

The method of modelling the delamination in composite beams and plates is versatile and allows analysis of the influence of multiple delaminations on natural frequencies of beams and plates with various boundary conditions. Using the elaborated models effects of location and size of delamination on bending natural frequencies of composite beams and plates were studied.

14. SUBJECT TERMS	15. NUMBER OF PAGES
Composite Materials. Craks and delamination	16. PRICE CODE

17. SECURITY CLASSIFICATION OF REPORT	18. SECURITY CLASSIFICATION OF THIS PAGE	19. SECURITY CLASSIFICATION OF ABSTRACT	20. LIMITATION OF ABSTRACT
UNCLASSIFIED	UNCLASSIFIED	UNCLASSIFIED	UL

Title of Research Project :

DYNAMICS OF CRACKED COMPOSITE MATERIALS STRUCTURES

Name of Principal Investigator :
Prof. Wiesław Ostachowicz

Name of Contractor :
Mary Ketelhut

Contract Number :
N68171-94-C-9108

The report number :
5th - final report

The report period :
15 August 1994 - 15 August 1995

The Research reported in this document has been made possible through the support and sponsorship of the U.S. Government through its European Research Office of the U.S. Army. This report is intended only for the internal management use of the Contractor and U.S. Government.

Abstract:

As a result of this work models of the finite beam and plate elements have been elaborated, to enable the analysis of the influence of the fatigue cracks and delaminations on the dynamic characteristics of the constructions made of unidirectional composite materials. The method of modelling the crack or delamination presented in the report enables an easy modification of the elaborated elements according to its specific damage (oblique crack, two-side crack, inside crack, multiple delaminations, etc.).

The results of numerical calculations obtained from the crack model are in consistence with the known influence of the position and depth of the crack on the decrease of the natural bending frequencies of the cantilever beam. Simultaneously, a strong influence of the material parameters on these changes has been observed, which does not exist in the case of isotropic materials.

The method of modelling the delamination in composite beams and plates is versatile and allows analysis of the influence of multiple delaminations on natural frequencies of beams and plates with various boundary conditions. Using the elaborated models effects of location and size of delamination on bending natural frequencies of composite beams and plates were studied.

DYNAMICS OF CRACKED COMPOSITE MATERIAL STRUCTURES

Grant No. N68171-94-C-9108

supported by European Research Office US Army

(Final Report)

W.Ostachowicz, M.Krawczuk, A.Żak
Institute of Fluid Flow Machinery
Polish Academy of Sciences
80-952 Gdańsk, Ul. Fiszera 14, Poland

1. Introduction

The use of composite materials in various construction elements has substantially increased over the past few years. These materials are particularly widely used in situations where a large strength-to-weight ratio is required. Composite materials similarly to isotropic materials are subjected to various damages, mostly cracks and delaminations. They result in local changes of the stiffness of the element made of such type of materials and consequently of its dynamic characteristics are altered. Changes of natural frequencies and mode shapes, amplitudes of forced vibrations and also coupling of vibrations forms are observed. The dynamic characteristics of damaged elements can be correlated with the location and size of damages [1-4] (cracks or delaminations). These relations are frequently used in diagnosis of such constructional elements - for example [5-8].

The problem of changes in dynamic characteristic of constructional elements with damages made of isotropic materials has been a subject of many papers, the review of which is given by Wauer [9], but only a limited number of papres have been devoted to the changes in the dynamic characteristics of composite constructional elements. Adams

et al. [10], found that damage in specimens fabricated from fibre reinforced plastics could be detected by a reduction in the natural frequencies and an increase in damping. Cawley and Adams [11], successfully tested the frequency measurement principle on composite matrix for unidirectional composite materials in the presence of damage. Nikpour and Dimarogonas [12], presented the local compliance matrix for unidirectional composite materials. They have shown that the interlocking deflection modes are enhanced as a function of the degree of anisotropy in composites. The effect of cracks upon the buckling of an edge-notched column for isotropic and anisotropic composites has been studied by Nikpour [13]. He indicated that the instability increases with the column slenderness and the crack length. In addition he has shown that the material anisotropy conspicuously reduces the load-carrying capacity of an externally cracked member. Manivasagam and Chandrasekaran [14] have presented the results of experimental investigations upon the reduction effect of the fundamental frequency of layered composite materials with damage in the form of cracks. The effects of delamination on buckling and post-buckling deformation and delamination growth with various geometrical parameters, loading conditions, material properties and boundary conditions have been studied extensively by Chai *et al.* [15], Bottega and Maewal [16], Whitcomb [17], Yin *et al.* [18] and Chen [19]. However, only a few investigations have been conducted to study the effect of delamination on vibration characteristics. Natural frequencies of delaminated beams have been studied by Ramkumar *et al.* [20] on the basis of the Timoshenko beam theory. The authors, however, did not take into account the effect of coupling of the transverse vibration with the longitudinal wave motion in the upper and lower split layers. Their analytical results predicted significant reduction of the fundamental frequency (from that of the perfect beam) and this prediction was found to disagree with the experimental observation. Wang *et al.* [21] used the classical beam theory but they considered the coupling effect. With the inclusion of coupling, the calculated fundamental frequency was not appreciably reduced by the presence of a relatively short delamination and the results were in close agreement with experimental measurements. The effect of delamination upon the natural frequencies and mode shapes

was analysed by Shen and Grady [22]. The effect of coupling between longitudinal and bending vibrations was considered in their model. Free vibration of a laminated composite beam-plate with a one dimensional delamination with respect to postbuckled reference states was also studied by Yin and Jane [23].

It is characteristic for all cited papers that their authors applied a continuos or discrete continuos models i.e. models which are based on differential equations. The crack in such models was substituted by a spring with additional boundary conditions [12-13] or by reduction in elastic modulus of material - see for more details [10-11]. The delamination was modelled by additional boundary conditions - see for more details [22]. This method of modelling is inconvenient for more realistic structures than beams or plates with constant cross-section. For this reason the authors of the presented report elaborated the alternative techniques of modelling of damaged structures. This technique is based on finite element method. The report presented the formulation of characteristic matrices for beam finite element with the transverse crack and delamination and also for the plate finite element with delamination. The results of numerical calculations received on the basis of elaborated models are also presented in the report.

2. Cracked beam finite element

2.1. General description of the element

In the Fig.2.1 a composite beam finite element with the transverse crack is presented. The cracks is placed in the middle of the element and remains open, its depth is a. The width of the element is B, the length L and the height H. The angle between the fibre and the axis of the element (plane perpendicular to the crack) is α. The element has three nodes (I, II, III). Each of them has two degrees of freedom: transverse displacements q_1, q_3, q_5 and rotations q_2, q_4, q_6. Considering only the case of flat

bending, and assuming that there is no warping in the transverse cross-section of the element, displacements on the both sides of the element could be expressed by relations:

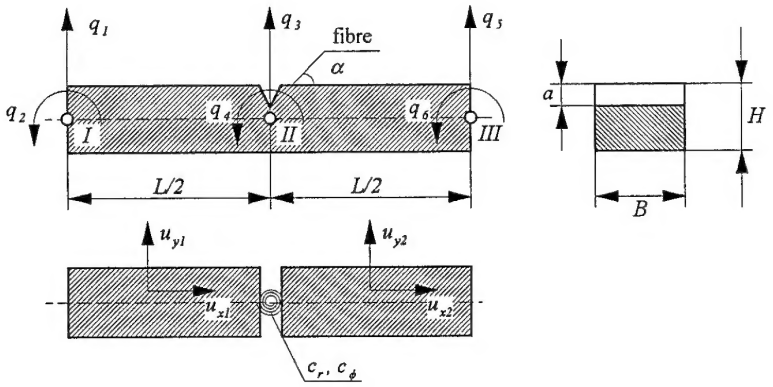

Fig.2.1 Composite beam finite element with a transverse crack.

$$\begin{cases} u_{x1}(x,y) = -y \cdot \phi_1(x) \\ u_{y1}(x,y) = v_1(x) \end{cases}, \quad \begin{cases} u_{x2}(x,y) = -y \cdot \phi_2(x) \\ u_{y2}(x,y) = v_2(x) \end{cases} \tag{2.1}$$

where ϕ_i $(i = 1, 2)$ denotes rotation and v_i $(i = 1, 2)$ - transverse displacement. Transverse displacements v_i on both sides of the crack (on left and right hand side of the element) could be approximated by cubic polynomials while the independent rotations ϕ_i by quadratic polynomials [24]:

$$\begin{cases} v_1(x) = a_1 + a_2 x + a_3 x^2 + a_4 x^3 \\ \phi_1(x) = a_5 + a_6 x + a_7 x^2 \end{cases}, \quad \begin{cases} v_2(x) = a_8 + a_9 x + a_{10} x^2 + a_{11} x^3 \\ \phi_2(x) = a_{12} + a_{13} x + a_{14} x^2 \end{cases} \tag{2.2}$$

Assuming that the distribution of the shear stress is linear [25], the relations (2.2) could be written in the form:

$$\begin{cases} v_1(x) = a_1 + a_2 x + a_3 x^2 + a_4 x^3 \\ \phi_1(x) = a_5 + a_6 x + 3a_4 x^2 \end{cases}, \quad \begin{cases} v_2(x) = a_7 + a_8 x + a_9 x^2 + a_{10} x^3 \\ \phi_2(x) = a_{11} + a_{12} x + 3a_{10} x^2 \end{cases} \tag{2.2.a}$$

Using the conditions in the nodes of the element and the conditions expressing consistency of displacements in x and y directions, and the balance of forces and

moments we could obtain the unknown values $a_1 - a_{12}$. Values c_r and c_ϕ represent flexibility coefficients of the element in the crack.

$$
\begin{aligned}
&v_1(x=0) = q_1\ , \qquad \phi_1(x=0) = q_2 \\
&v_1(x=L/2) = q_3\ , \qquad \phi_1(x=L/2) = q_4 \\
&v_2(x=L) = q_5\ , \qquad \phi_2(x=L) = q_6 \\
&u_{x1}(x=L/2) - u_{x2}(x=L/2) = c_r \cdot u'_{x1}(x=L/2) \\
&u'_{x1}(x=L/2) = u'_{x2}(x=L/2) \\
&u_{y1}(x=L/2) = u_{y2}(x=L/2) \\
&u'_{y1}(x=L/2) - u'_{y2}(x=L/2) = c_\phi \cdot u''_{y1}(x=L/2) \\
&u''_{y1}(x=L/2) = u''_{y2}(x=L/2) \\
&u'''_{y1}(x=L/2) = u'''_{y2}(x=L/2)
\end{aligned}
\tag{2.3}
$$

Applying the standard finite element formula the coefficients $a_1 - a_{12}$ could be written as:

$$
\begin{Bmatrix} a_1 \\ \vdots \\ a_6 \end{Bmatrix} = \mathbf{A}_1 \begin{Bmatrix} q_1 \\ \vdots \\ q_6 \end{Bmatrix}, \quad \begin{Bmatrix} a_7 \\ \vdots \\ a_{12} \end{Bmatrix} = \mathbf{A}_2 \begin{Bmatrix} q_1 \\ \vdots \\ q_6 \end{Bmatrix} \tag{2.4}
$$

where matrices $\mathbf{A}_1$ and $\mathbf{A}_2$ take the following form:

$$
\mathbf{A}_1 = \begin{bmatrix}
1 & 0 & 0 & 0 & 0 & 0 \\
-\dfrac{3L-4c_\phi}{\tilde{\alpha}L} & \dfrac{L-2c_r}{3\tilde{\beta}} & \dfrac{4(L-c_\phi)}{\tilde{\alpha}L} & -\dfrac{2}{3} & -\dfrac{1}{\tilde{\alpha}} & \dfrac{L}{3\tilde{\beta}} \\
\dfrac{2}{\tilde{\alpha}L} & -\dfrac{L-2c_r}{\tilde{\beta}L} & -\dfrac{4}{\tilde{\alpha}L} & \dfrac{2}{L} & \dfrac{2}{\tilde{\alpha}L} & -\dfrac{1}{\tilde{\beta}} \\
0 & \dfrac{2(L-2c_r)}{3\tilde{\beta}L^2} & 0 & -\dfrac{4}{3L^2} & 0 & \dfrac{2}{3\tilde{\beta}L} \\
0 & 1 & 0 & 0 & 0 & 0 \\
0 & -\dfrac{3L-4c_r}{\tilde{\beta}L} & 0 & \dfrac{4}{L} & 0 & -\dfrac{1}{\tilde{\beta}}
\end{bmatrix}
\tag{2.5}
$$

$$\mathbf{A}_2 = \begin{bmatrix} \frac{L}{\tilde{\alpha}} & 0 & -\frac{4c_\phi}{\tilde{\alpha}} & 0 & \frac{2c_\phi}{\tilde{\alpha}} & 0 \\ -\frac{3}{\tilde{\alpha}} & \frac{L-2c_r}{3\tilde{\beta}} & \frac{4(L+c_\phi)}{\tilde{\alpha}L} & -\frac{2}{3} & -\frac{L+4c_\phi}{\tilde{\alpha}L} & \frac{L}{3\tilde{\beta}} \\ \frac{2}{\tilde{\alpha}L} & -\frac{L-2c_r}{\tilde{\beta}L} & -\frac{4}{\tilde{\alpha}L} & \frac{2}{L} & \frac{2}{\tilde{\alpha}L} & -\frac{1}{\tilde{\beta}} \\ 0 & \frac{2(L-2c_r)}{3\tilde{\beta}L^2} & 0 & -\frac{4}{3L^2} & 0 & \frac{2}{3\tilde{\beta}L} \\ 0 & \frac{L}{\tilde{\beta}} & 0 & 0 & 0 & \frac{c_r}{\tilde{\beta}} \\ 0 & -\frac{3L-4c_r}{\tilde{\beta}L} & 0 & \frac{4}{L} & 0 & -\frac{1}{\tilde{\beta}} \end{bmatrix} \tag{2.6}$$

where $\tilde{\alpha} = L - 2c_\phi, \tilde{\beta} = L - c_r$.

Next, from the relations between the coefficients $a_1 - a_{12}$ and the displacements we could easily obtain the relations for the shape function $\mathbf{N}_1$ and $\mathbf{N}_2$ in both parts of the element:

$$\begin{Bmatrix} u_{x1} \\ u_{y1} \end{Bmatrix} = \mathbf{N}_1 \begin{Bmatrix} q_1 \\ \vdots \\ q_6 \end{Bmatrix}, \quad \begin{Bmatrix} u_{x2} \\ u_{y2} \end{Bmatrix} = \mathbf{N}_2 \begin{Bmatrix} q_7 \\ \vdots \\ q_{12} \end{Bmatrix} \tag{2.7}$$

$$\mathbf{N}_1 = \mathbf{X}_1 \cdot \mathbf{A}_1, \quad \mathbf{N}_1 = \mathbf{X}_1 \cdot \mathbf{A}_1 \tag{2.7.a}$$

where matrices $\mathbf{X}_1$ and $\mathbf{X}_2$ have the form:

$$\mathbf{X}_1 = \mathbf{X}_2 = \begin{bmatrix} 0 & 0 & 0 & -3x^2y & -y & -xy \\ 1 & x & x^2 & x^3 & 0 & 0 \end{bmatrix} \tag{2.8}$$

The strains in the element could be obtained from the following relations:

$$\begin{cases} \varepsilon_{x1}(x,y) = -y\dfrac{\partial \phi_1(x)}{\partial x} \\ \gamma_{x1y1}(x,y) = \dfrac{\partial v_1(x)}{\partial x} - \phi_1(x) \end{cases}, \quad \begin{cases} \varepsilon_{x2}(x,y) = -y\dfrac{\partial \phi_2(x)}{\partial x} \\ \gamma_{x2y2}(x,y) = \dfrac{\partial v_2(x)}{\partial x} - \phi_2(x) \end{cases} \tag{2.9}$$

Substituting the relations (2.2.a) into equations (2.9) and using the relations (2.4), (2.5), and (2.6), the strains inside the elements could be expressed in the node–displacement

function. It means, that the linear strain-nodal displacement relation matrices $\mathbf{B}_1$ and $\mathbf{B}_2$ have the form:

$$\begin{Bmatrix} \varepsilon_{x1} \\ \gamma_{x1y1} \end{Bmatrix} = \mathbf{B}_1 \begin{Bmatrix} q_1 \\ \vdots \\ q_6 \end{Bmatrix}, \quad \begin{Bmatrix} \varepsilon_{x2} \\ \gamma_{x2y2} \end{Bmatrix} = \mathbf{B}_2 \begin{Bmatrix} q_7 \\ \vdots \\ q_{12} \end{Bmatrix} \tag{2.10}$$

$$\mathbf{B}_1 = \tilde{\mathbf{X}}_1 \cdot \mathbf{A}_1, \quad \mathbf{B}_2 = \tilde{\mathbf{X}}_2 \cdot \mathbf{A}_2 \tag{2.10.a}$$

where matrices $\tilde{\mathbf{X}}_1$ and $\tilde{\mathbf{X}}_2$ denote:

$$\tilde{\mathbf{X}}_1 = \tilde{\mathbf{X}}_2 = \begin{bmatrix} 0 & 0 & 0 & -6xy & 0 & -y \\ 0 & 1 & 2x & 0 & -1 & -x \end{bmatrix} \tag{2.11}$$

Finally, the matrix of inertia and stiffness matrix of transverse cracked element could be written in the following form:

$$\begin{aligned} \mathbf{M}_e &= \rho \int_{V_1} \mathbf{N}_1^T \mathbf{N}_1 dV_1 + \rho \int_{V_1} \mathbf{N}_2^T \mathbf{N}_2 dV_2 = \\ &= \rho \mathbf{A}_1^T \int_{V_1} \mathbf{X}_1^T \mathbf{X}_1 dV_1 \mathbf{A}_1 + \rho \mathbf{A}_2^T \int_{V_1} \mathbf{X}_2^T \mathbf{X}_2 dV_2 \mathbf{A}_2 = \\ &= \rho \mathbf{A}_1^T \tilde{\mathbf{M}}_e^1 \mathbf{A}_1 + \rho \mathbf{A}_2^T \tilde{\mathbf{M}}_e^2 \mathbf{A}_2 \end{aligned} \tag{2.12}$$

$$\begin{aligned} \mathbf{K}_e &= \int_{V_1} \mathbf{B}_1^T \mathbf{D} \mathbf{B}_1 dV_1 + \int_{V_1} \mathbf{B}_2^T \mathbf{D} \mathbf{B}_2 dV_2 = \\ &= \mathbf{A}_1^T \int_{V_1} \tilde{\mathbf{X}}_1^T \tilde{\mathbf{X}}_1 dV_1 \mathbf{A}_1 + \mathbf{A}_2^T \int_{V_1} \tilde{\mathbf{X}}_2^T \tilde{\mathbf{X}}_2 dV_2 \mathbf{A}_2 = \\ &= \mathbf{A}_1^T \tilde{\mathbf{K}}_e^1 \mathbf{A}_1 + \mathbf{A}_2^T \tilde{\mathbf{K}}_e^2 \mathbf{A}_2 \end{aligned} \tag{2.13}$$

where matrix $\mathbf{D}$ is the stress-strain relation matrix for the unidirectional composite material. Substituting into equations (2.12) and (2.13) relations (2.5) and (2.6) and after multiplying and integrating, the inertia and stiffness matrices for both parts of the element take the following form:

$$\tilde{\mathbf{M}}_e^1 = BHL\begin{bmatrix} \frac{1}{2} & \frac{L}{8} & \frac{L^2}{24} & \frac{L^3}{64} & 0 & 0 \\ & \frac{L^2}{24} & \frac{L^3}{64} & \frac{L^4}{160} & 0 & 0 \\ & & \frac{L^4}{160} & \frac{L^5}{384} & 0 & 0 \\ & & & \frac{L^6}{896}+\frac{3L^4H^2}{640} & \frac{L^2H^2}{96} & \frac{L^3H^2}{256} \\ & \text{Sym.} & & & \frac{H^2}{24} & \frac{LH^2}{96} \\ & & & & & \frac{L^2H^2}{288} \end{bmatrix} \tag{2.14}$$

$$\tilde{\mathbf{M}}_e^2 = BHL\begin{bmatrix} \frac{1}{2} & \frac{3L}{8} & \frac{7L^2}{24} & \frac{15L^3}{64} & 0 & 0 \\ & \frac{7L^2}{24} & \frac{15L^3}{64} & \frac{31L^4}{160} & 0 & 0 \\ & & \frac{31L^4}{160} & \frac{21L^5}{128} & 0 & 0 \\ & & & \frac{127L^6}{896}+\frac{93L^4H^2}{640} & \frac{7L^2H^2}{96} & \frac{15L^3H^2}{256} \\ & \text{Sym.} & & & \frac{H^2}{24} & \frac{LH^2}{96} \\ & & & & & \frac{7L^2H^2}{288} \end{bmatrix} \tag{2.15}$$

$$\tilde{\mathbf{K}}_e^1 = BHL\begin{bmatrix} 0 & 0 & 0 & 0 & 0 & 0 \\ & \frac{S_{66}}{2} & \frac{LS_{66}}{4} & 0 & -\frac{S_{66}}{2} & -\frac{LS_{66}}{8} \\ & & \frac{L^2S_{66}}{6} & 0 & -\frac{LS_{66}}{4} & -\frac{L^2S_{66}}{12} \\ & & & \frac{L^2H^2S_{11}}{8} & 0 & \frac{LH^2S_{11}}{8} \\ & \text{Sym.} & & & \frac{S_{66}}{2} & \frac{LS_{66}}{8} \\ & & & & & \frac{L^2S_{66}+H^2S_{11}}{24} \end{bmatrix} \tag{2.16}$$

$$\tilde{\mathbf{K}}_e^2 = BHL\begin{bmatrix} 0 & 0 & 0 & 0 & 0 & 0 \\ & \frac{S_{66}}{2} & \frac{3LS_{66}}{4} & 0 & -\frac{S_{66}}{2} & -\frac{3LS_{66}}{8} \\ & & \frac{7L^2S_{66}}{6} & 0 & -\frac{3LS_{66}}{4} & -\frac{7L^2S_{66}}{12} \\ & & & \frac{7L^2H^2S_{11}}{8} & 0 & \frac{3LH^2S_{11}}{16} \\ & \text{Sym.} & & & \frac{S_{66}}{2} & \frac{3LS_{66}}{8} \\ & & & & & \frac{7L^2S_{66}+H^2S_{11}}{24} \end{bmatrix} \tag{2.17}$$

where S_{11} and S_{66} are the elements of the stress-strain relation matrix (see Appendix C).

2.2. The model and the algorithm for calculating the flexibility in the crack

The flexibility coefficients of the element due to the appearance of the crack could be obtained from the Castigliano theorem:

$$c_{ij} = \frac{\partial^2 U}{\partial P_i \, \partial P_j} \tag{2.18}$$

where U is the additional elastic strain energy of the element caused by the crack, while P_i and P_j denote the independent nodal forces of the finite element. The additional elastic strain energy in the case of cracks existing in the unidirectional composite materials [12] equals to:

$$U = \int_A \left\{ D_1 \sum_{i=1}^{n} K_{Ii}^2 + D_{12} \sum_{i=1}^{n} K_{Ii} \sum_{j=1}^{n} K_{IIj} + D_2 \sum_{i=1}^{n} K_{IIi}^2 \right\} dA \tag{2.19}$$

where A is the surface of the crack, K_{ji} $(j = I, II, i = 1, 2, ..., n)$ are the stress intensity factors and D_1, D_{12}, D_2 are the coefficients depending on the material parameters.

$$D_1 = -0.5\bar{b}_{22}\,\mathrm{Im}\left[1/s_1 + 1/s_1\right]$$
$$D_{12} = \bar{b}_{11}\,\mathrm{Im}\left[s_1 s_2\right] \tag{2.20}$$
$$D_2 = 0.5\bar{b}_{11}\,\mathrm{Im}\left[s_1 + s_2\right]$$

The formulae for calculating values s_1, s_2 and $\bar{b}_{ij}$ are shown in Appendix B.

In the general case, stress intensity factors for composite materials are not equal to the stress intensity factors calculated from the solution of the crack problem of the same geometry in the isotropic material. According to the results presented in the paper [26] these factors could be written as:

$$K_{ji} = \sigma_i \sqrt{\pi a} F_{ji}\left(a/H, \sqrt[4]{\lambda} L/H, \zeta\right) \tag{2.21}$$

where σ_i denotes the stress acting in the crack, a is the depth of the crack, H is the height of the element, F_{ji} are the correction factors, which consider the finite dimensions of the element and properties of the material (anisotropy of the material), while the material parameters λ, ζ are given in paper [26]. It is also shown there, that for $\sqrt[4]{\lambda} L/H > 2$ intensity factors for transverse cracks in composite materials could be given as:

$$K_{ji} = \sigma_i \sqrt{\pi a} F_{ji}(a/H) Y_j(\zeta) \tag{2.22}$$

where $Y_j(\zeta)$ is the correction function which takes into consideration the anisotropy of the material [26].

Finally, we obtain:

$$c_r = \frac{2\pi D_1}{B} \int_0^{\tilde{\xi}} (F_1 Y_1)^2 \, \xi \, d\xi \tag{2.23.a}$$

$$c_\phi = \frac{72\pi D_1}{BH^2} \int_0^{\tilde{\xi}} (F_2 Y_1)^2 \, \xi \, d\xi \tag{2.23.b}$$

where from [26]:

$$F_1 = \sqrt{\frac{\tan\eta}{\eta}} \frac{0.752 + 2.02\xi + 0.37(1 - \sin\eta)^3}{\cos\eta} \tag{2.24.a}$$

$$F_2 = \sqrt{\frac{\tan\eta}{\eta}}\,\frac{0.923+0.199(1-\sin\eta)^4}{\cos\eta} \tag{2.24.b}$$

$$Y_1 = 1+0.1(\zeta-1)-0.016(\zeta-1)^2+0.002(\zeta-1)^3 \tag{2.24.c}$$

$$\zeta = \frac{\sqrt{E_{11}E_{22}}}{2G_{12}} - \nu_{12}\sqrt{\frac{E_{22}}{E_{11}}} \tag{2.24.d}$$

and $\xi = a/H$, $\eta = \pi a/2H$, while B is the width of the element. The method of calculating of the material parameters is shown in Appendix A.

3. Delaminated beam finite element

3.1. General description of the element

A discrete model of a delaminated part of the beam is presented in Fig.3.1 The delaminated region is modelled by three beam finite elements which are connected at the tip of the delamination by additional boundary conditions.

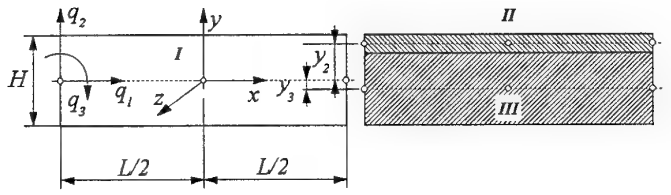

Fig.3.1. The delaminated region of a beam modelled by finite elements.

The layers are located symmetrically with respect to the x-z plane. Each element has three nodes at $x = -L/2$, $x = 0$, $x = L/2$. At each node there are three degrees of freedom which are axial displacement q_1, q_4, q_7, transverse displacement q_3, q_6, q_9 and the independent rotation q_2, q_5, q_8. Additionally it is assumed that the number of degrees of freedom is independent of the number of layers.

3.1.1. Description of the element number *I*

Neglecting warping, the displacements u and v of a point can be expressed as:

$$\begin{cases} u(x,y) = u^0(x) - y \cdot \phi(x) \\ v(x,y) = v^0(x) \end{cases} \tag{3.1}$$

where $u^0(x)$ denotes the axial displacement, $\phi(x)$ the independent rotation, and $v^0(x)$ the transverse displacement.

In the finite-element modelling, the bending displacements $v^0(x)$ are assumed to be cubic polynomials in x, while the axial displacement $u^0(x)$ and the rotation $\phi(x)$ are assumed to be quadratic. Additionally it is assumed that shear strain variation is linear, as proposed by Tessler and Dong [25]. Employing the above conditions, the displacements and rotation in the element may be written in the following forms:

$$\begin{cases} u^0(x) = a_1 + a_2 x + a_3 x^2 \\ \phi(x) = a_4 + a_5 x + 3a_9 x^2 \\ v^0(x) = a_6 + a_7 x + a_8 x^2 + a_9 x^3 \end{cases} \tag{3.2}$$

The constants $a_1 - a_9$ can be expressed in terms of the element degrees of freedom by using the nodal conditions in the following forms:

$$\begin{aligned} &u^0(x = -L/2) = q_1 \\ &\phi(x = -L/2) = q_2 \\ &v^0(x = -L/2) = q_3 \\ &u^0(x = 0) = q_4 \\ &\phi\ (x = 0) = q_5 \\ &v^0(x = 0) = q_6 \\ &u^0(x = L/2) = q_7 \\ &\phi\ (x = L/2) = q_8 \\ &v^0(x = L/2) = q_9 \end{aligned} \tag{3.3}$$

Finally we obtain:

$$
\begin{aligned}
a_1 &= q_4 \\
a_2 &= \frac{-q_1 + q_7}{L} \\
a_3 &= \frac{2(q_1 - 2q_4 + q_7)}{L^2} \\
a_4 &= q_6 \\
a_5 &= \frac{-q_3 + q_9}{L} \\
a_6 &= q_5 \\
a_7 &= \frac{-6q_2 - q_3 L + 2q_6 L + 6q_8 - q_9 L}{6L} \\
a_8 &= \frac{2(q_2 - 2q_5 + q_8)}{L^2} \\
a_9 &= \frac{2(q_3 - 2q_6 + q_9)}{3L^2}
\end{aligned}
\tag{3.4}
$$

Taking into account Eqs. (3.4) and Eq. (3.2) we can determine the matrix of the shape function for the single layer of the element.

$$
\mathbf{N} = \mathbf{X} \cdot \mathbf{A} \tag{3.5}
$$

where matrix $\mathbf{X}$ has the form:

$$
\mathbf{X} = \begin{bmatrix} 1 & x & x^2 & -y & -xy & 0 & 0 & 0 & -3x^2 y \\ 0 & 0 & 0 & 0 & 0 & 1 & x & x^2 & x^3 \end{bmatrix} \tag{3.6}
$$

whereas the matrix $\mathbf{A}$ can be expressed as:

$$\mathbf{A}=\begin{bmatrix} 0 & 0 & 0 & 1 & 0 & 0 & 0 & 0 & 0 \\ -\frac{1}{L} & 0 & 0 & 0 & 0 & 0 & \frac{1}{L} & 0 & 0 \\ \frac{2}{L^2} & 0 & 0 & -\frac{4}{L^2} & 0 & 0 & \frac{2}{L^2} & 0 & 0 \\ 0 & 0 & 0 & 0 & 0 & 1 & 0 & 0 & 0 \\ 0 & 0 & -\frac{1}{L} & 0 & 0 & 0 & 0 & 0 & \frac{1}{L} \\ 0 & 0 & 0 & 0 & 1 & 0 & 0 & 0 & 0 \\ 0 & -\frac{1}{L} & -\frac{1}{6} & 0 & 0 & \frac{1}{3} & 0 & \frac{1}{L} & -\frac{1}{6} \\ 0 & \frac{2}{L^2} & 0 & 0 & -\frac{4}{L^2} & 0 & 0 & \frac{2}{L^2} & 0 \\ 0 & 0 & \frac{2}{3L^2} & 0 & 0 & -\frac{4}{3L^2} & 0 & 0 & \frac{2}{3L^2} \end{bmatrix} \tag{3.7}$$

Employing the shape function matrix for the single layer, we can determine the inertia matrix of the whole element using the following formula:

$$\begin{aligned} \mathbf{M}_e = \sum_{j=1}^{j=R} \mathbf{M}_e^j = \sum_{j=1}^{j=R} \rho_j \int_{V_j} \mathbf{N}^T \mathbf{N} dV_j = \sum_{j=1}^{j=R} \rho_j \mathbf{A}^T \int_{V_j} \mathbf{X}^T \mathbf{X} dV_j \mathbf{A} \\ = \sum_{j=1}^{j=R} \rho_j \mathbf{A}^T \tilde{\mathbf{M}}_e^j \mathbf{A} \end{aligned} \tag{3.8}$$

where j denotes the number of a layer, R the global number of layers in the element, V_j the volume of the j-th layer of material and ρ_j the density of the i-th layer.

The value of the integral in Eq. (3.8) (for the j-th layer) can be expressed in closed form as:

$$\tilde{\mathbf{M}}_e^j = BL\begin{bmatrix} \alpha & 0 & \frac{L^2}{12}\alpha & -\frac{1}{2}\beta & 0 & 0 & 0 & 0 & -\frac{L^2}{8}\beta \\ & \frac{L^2}{12}\alpha & 0 & 0 & -\frac{L^2}{24}\beta & 0 & 0 & 0 & 0 \\ & & \frac{L^4}{80}\alpha & -\frac{L^2}{24}\beta & 0 & 0 & 0 & 0 & -\frac{3L^4}{160}\beta \\ & & & \frac{1}{3}\gamma & 0 & 0 & 0 & 0 & \frac{L^2}{12}\gamma \\ & & & & \frac{L^2}{36}\gamma & 0 & 0 & 0 & 0 \\ & & & & & \alpha & 0 & \frac{L^2}{12}\alpha & 0 \\ & & & & & & \frac{L^2}{12}\alpha & 0 & \frac{L^4}{80}\alpha \\ & \text{Sym.} & & & & & & \frac{L^4}{80}\alpha & 0 \\ & & & & & & & & \frac{L^6}{448}\alpha+\frac{3L^4}{80}\gamma \end{bmatrix} \tag{3.9}$$

where $\alpha = H_{j+1} - H_j$, $\beta = H_{j+1}^2 - H_j^2$, $\gamma = H_{j+1}^3 - H_j^3$.

The strains of the single layer of material are given by the following formulas:

$$\begin{cases} \varepsilon_x = \dfrac{\partial u(x,y)}{\partial x} = \dfrac{\partial u^0(x)}{\partial x} - y\dfrac{\partial \phi(x)}{\partial x} \\ \gamma_{xy} = \dfrac{\partial u(x,y)}{\partial y} + \dfrac{\partial v(x,y)}{\partial x} = \dfrac{\partial v^0(x)}{\partial x} - \phi \end{cases} \tag{3.10}$$

Taking into account relations (3.2) and (3.4), the strains in the single layer can be expressed as a function of nodal degrees of freedom:

$$\begin{bmatrix} \varepsilon_x \\ \gamma_{xy} \end{bmatrix} = \mathbf{B} \cdot \begin{bmatrix} q_1 \\ q_2 \\ \vdots \\ q_9 \end{bmatrix} \tag{3.11}$$

where matrix **B** equals

$$\mathbf{B} = \tilde{\mathbf{X}} \cdot \mathbf{A} \tag{3.12}$$

and matrix $\tilde{\mathbf{X}}$ is given as:

$$\tilde{\mathbf{X}} = \begin{bmatrix} 0 & 1 & 2x & 0 & -y & 0 & 0 & 0 & -6xy \\ 0 & 0 & 0 & -1 & -x & 0 & 1 & 2x & 0 \end{bmatrix} \tag{3.13}$$

The stiffness matrix of the whole element has the form:

$$\begin{aligned} \mathbf{K}_e = \sum_{j=1}^{j=R} \mathbf{K}_e^j = \sum_{j=1}^{j=R} \int_{V_j} \mathbf{B}^T \mathbf{D}_j \mathbf{B}\, dV_j = \sum_{j=1}^{j=R} \mathbf{A}^T \int_{V_j} \tilde{\mathbf{X}}^T \mathbf{D}_j \tilde{\mathbf{X}}\, dV_j\, \mathbf{A} = \\ = \sum_{j=1}^{j=R} \mathbf{A}^T \tilde{\mathbf{K}}_e^j \mathbf{A} \end{aligned} \tag{3.14}$$

where $\mathbf{D}_j$ denotes the matrix which describes relations between stresses and strains in the j-th layer of the element (see Appendix C).

The values of the integral in Eq. (3.14) (for the j-th layer of the material) can be presented in closed form as:

$$\tilde{\mathbf{K}}_e^j = BL \begin{bmatrix} 0 & 0 & 0 & 0 & 0 & 0 & 0 & 0 & 0 \\ & S_{11}\alpha & 0 & -S_{16}\alpha & -\frac{S_{11}}{2}\beta & 0 & S_{16}\alpha & 0 & 0 \\ & & \frac{S_{11}L^2}{3}\alpha & 0 & -\frac{S_{16}L^2}{6}\alpha & 0 & 0 & \frac{S_{16}L^2}{3}\alpha & -\frac{S_{11}L^2}{2}\beta \\ & & & S_{66}\alpha & \frac{S_{16}}{2}\beta & 0 & -S_{66}\alpha & 0 & 0 \\ & & & & \frac{S_{66}L^2\alpha + 4S_{11}\gamma}{12} & 0 & -\frac{S_{66}L^2}{6}\alpha & -\frac{S_{66}L^2}{6}\alpha & 0 \\ & & & & & 0 & 0 & 0 & 0 \\ & & & & & & S_{66}\alpha & 0 & 0 \\ & \text{Sym.} & & & & & & \frac{S_{66}L^2}{3}\alpha & -\frac{S_{16}L^2}{2}\beta \\ & & & & & & & & S_{11}L^2\gamma \end{bmatrix} \tag{3.15}$$

where $\alpha = H_{j+1} - H_j$, $\beta = H_{j+1}^2 - H_j^2$, $\gamma = H_{j+1}^3 - H_j^3$.

3.1.2. Description of elements number *II* and *III*

In order to connect element *I* with elements *II* and *III*, the following boundary conditions are applied at the tip of the delamination:

$$\begin{cases} u_1^0(x) = u_2^0(x) + z_2\phi_2(x) \\ u_1^0(x) = u_3^0(x) + z_3\phi_3(x) \\ \phi_1(x) = \phi_2(x) = \phi_3(x) \\ v_1^0(x) = v_2^0(x) = v_3^0(x) \end{cases} \tag{3.16}$$

where z_2 and z_3 denote distances between neutral axes of elements *I-II* and *I-III*, respectively (see Fig.3.1).

Taking into account relations (3.16) and (3.2), the relationships between constants $a_1 - a_9$ for the above-mentioned elements can be evaluated as:

$$\begin{cases} a_4^I = a_4^{II} = a_4^{III}, \quad a_5^I = a_5^{II} = a_5^{III} \\ a_6^I = a_6^{II} = a_6^{III}, \quad a_7^I = a_7^{II} = a_7^{III} \\ a_8^I = a_8^{II} = a_8^{III}, \quad a_9^I = a_9^{II} = a_9^{III} \end{cases} \tag{3.17.a}$$

$$\begin{cases} a_1^{II} = a_1^I - y_2 a_4^I, \quad a_1^{III} = a_1^I - y_3 a_4^I \\ a_2^{II} = a_2^I - y_2 a_5^I, \quad a_2^{III} = a_2^I - y_3 a_5^I \\ a_3^{II} = a_3^I - 3y_2 a_9^I, \quad a_3^{III} = a_3^I - 3y_3 a_9^I \end{cases} \tag{3.17.b}$$

where the superscripts *I*, *II* and *III* denote the number of the element in the region of delamination.

The shape function matrices for the elements number *II* and *III* will have the following forms:

$$\mathbf{N}_2 = \mathbf{X} \cdot \mathbf{A}_2 \tag{3.18}$$

$$\mathbf{N}_3 = \mathbf{X} \cdot \mathbf{A}_3 \tag{3.19}$$

where $\mathbf{A}_i$ $(i = 1, 2)$:

$$\mathbf{A}_i = \begin{bmatrix} 0 & 0 & 0 & 1 & 0 & z_i & 0 & 0 & 0 \\ -\frac{1}{L} & 0 & \frac{z_i}{L} & 0 & 0 & 0 & \frac{1}{L} & 0 & -\frac{z_i}{L} \\ \frac{2}{L^2} & 0 & -\frac{2z_i}{L^2} & -\frac{4}{L^2} & 0 & \frac{4z_i}{L^2} & \frac{2}{L^2} & 0 & -\frac{2z_i}{L^2} \\ 0 & 0 & 0 & 0 & 0 & 1 & 0 & 0 & 0 \\ 0 & 0 & -\frac{1}{L} & 0 & 0 & 0 & 0 & 0 & \frac{1}{L} \\ 0 & 0 & 0 & 0 & 1 & 0 & 0 & 0 & 0 \\ 0 & -\frac{1}{L} & -\frac{1}{6} & 0 & 0 & \frac{1}{3} & 0 & \frac{1}{L} & -\frac{1}{6} \\ 0 & \frac{2}{L^2} & 0 & 0 & -\frac{4}{L^2} & 0 & 0 & \frac{2}{L^2} & 0 \\ 0 & 0 & \frac{2}{3L^2} & 0 & 0 & -\frac{4}{3L^2} & 0 & 0 & \frac{2}{3L^2} \end{bmatrix} \tag{3.20}$$

Taking into account matrices $\mathbf{A}_2$ and $\mathbf{A}_3$ we can determine (using relation 3.8) the inertia matrix of elements *II* and *III*.

In a similar way matrices $\mathbf{B}_2$ and $\mathbf{B}_3$ of elements *II* and *III* can be evaluated, and finally the stiffness matrices (using relation 3.14) of these elements can be calculated.

4. Delaminated plate finite element

4.1. General description

The way of modelling delaminated region in a composite plate with delamination is presented in Fig.4.1. The delamination is modelled by three plate finite elements. In order to connect these elements in the delamination crack tip, additional boundary conditions are applied. Material layers in an element are located symmetrically with respect to *x-y* plane. Each element has eight nodes with five degrees of freedom.

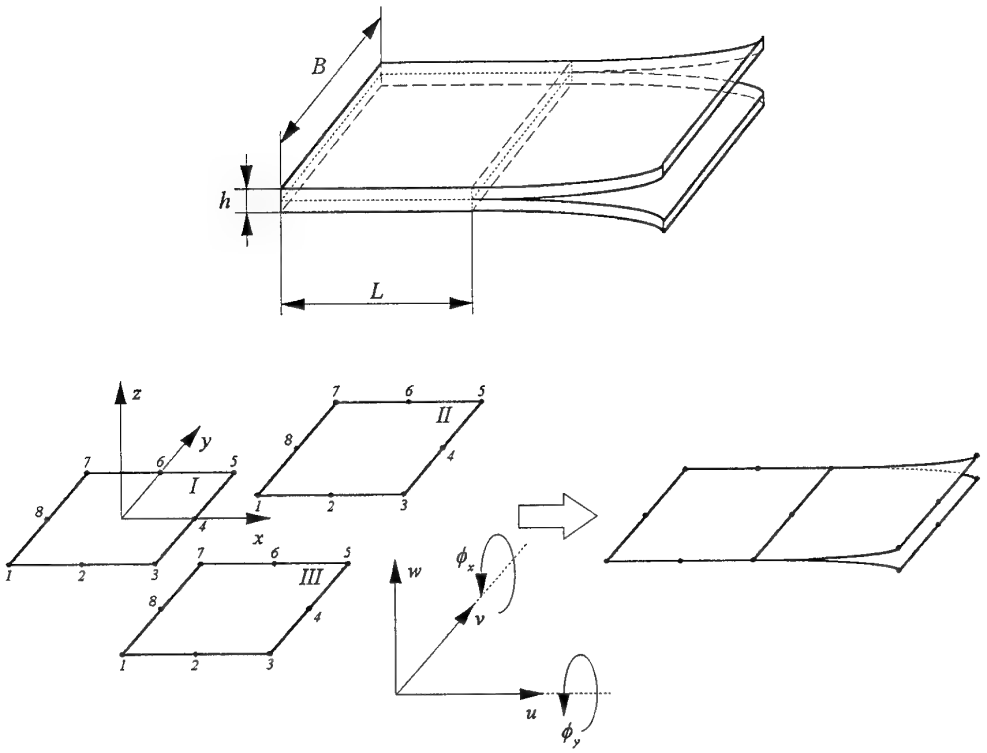

Fig. 4.1. The region of delamination in a plate modelled by finite elements.

Axial displacements u, v and w in a single layer can be expressed as:

$$\begin{cases} u(x,y,z) = u^0(x,y) - z \cdot \phi_x(x,y) \\ v(x,y,z) = v^0(x,y) - z \cdot \phi_y(x,y) \\ w(x,y,z) = w^0(x,y) \end{cases} \tag{4.1}$$

where u^0, v^0, w^0 denote mid-plane displacements, while ϕ_x and ϕ_y denote independent rotations. To approximate the axial mid-plane displacements and rotations biquadratic shape functions for eight-node element have been used.

$$\begin{Bmatrix} u \\ w \\ w \end{Bmatrix} = \mathbf{N}_{3x40} \cdot \begin{Bmatrix} q_1 \\ \vdots \\ q_{40} \end{Bmatrix} \tag{4.2}$$

$$
\begin{aligned}
N_1(\xi,\eta) &= -1/4+\xi^2-\xi\eta+\eta^2+2\xi^2\eta-2\xi\eta^2\\
N_2(\xi,\eta) &= 1/2+\eta-2\xi^2-4\xi^2\eta\\
N_3(\xi,\eta) &= -1/4+\xi^2+\xi\eta+\eta^2+2\xi^2\eta+2\xi\eta^2\\
N_4(\xi,\eta) &= 1/2-\xi-2\eta^2+4\xi\eta^2\\
N_5(\xi,\eta) &= 1/2+\xi-2\eta^2-4\xi\eta^2\\
N_6(\xi,\eta) &= -1/4+\xi^2+\xi\eta+\eta^2-2\xi^2\eta-2\xi\eta^2\\
N_7(\xi,\eta) &= 1/2-\eta-2\xi^2+4\xi^2\eta\\
N_8(\xi,\eta) &= -1/4+\xi^2-\xi\eta+\eta^2-2\xi^2\eta+2\xi\eta^2
\end{aligned}
\tag{4.2.a}
$$

where $\xi = x/L$ and $\eta = y/B$.

Using standard finite element formulae the inertia matrix of the whole element can be determined:

$$
\mathbf{M}_e = \sum_{j=1}^{j=R} \mathbf{M}_e^j = \sum_{j=1}^{j=R} \rho_j \int_{V_j} \mathbf{N}^T \mathbf{N}\, dV_j \tag{4.3}
$$

where j denotes the number of the layer, R total number of layers in the element, V_j the volume of the j-th layer of material and ρ_j the density of j-th layer.

The strains in the single layer of material can be calculated from the following relations:

$$
\begin{aligned}
\varepsilon_x &= \varepsilon_x^0 + z\cdot\kappa_x = \frac{\partial u^0}{\partial x} - z\frac{\partial \phi_x}{\partial x}\\
\varepsilon_y &= \varepsilon_y^0 + z\cdot\kappa_y = \frac{\partial v^0}{\partial y} - z\frac{\partial \phi_y}{\partial y}\\
\gamma_{xy} &= \gamma_{xy}^0 + z\cdot\kappa_{xy} = \left(\frac{\partial u^0}{\partial y}+\frac{\partial v^0}{\partial x}\right) - z\left(\frac{\partial \phi_x}{\partial y}+\frac{\partial \phi_y}{\partial x}\right)\\
\gamma_{xz} &= \frac{\partial w^0}{\partial x} - \phi_x\\
\gamma_{yz} &= \frac{\partial w^0}{\partial y} - \phi_y
\end{aligned}
\tag{4.4}
$$

Taking into account relations (4.1), (4.2) and (4.4) the strain in a single layer can be expressed in the following form:

$$\begin{Bmatrix} \varepsilon_x \\ \varepsilon_y \\ \gamma_{xy} \\ \gamma_{xz} \\ \gamma_{yz} \end{Bmatrix} = \mathbf{B}_{5\times 40} \cdot \begin{Bmatrix} q_1 \\ \vdots \\ q_{40} \end{Bmatrix} \tag{4.5}$$

Thus the stiffness matrix of the whole element can be written as:

$$\mathbf{K}_e = \sum_{j=1}^{j=R} \mathbf{K}_e^j = \sum_{j=1}^{j=R} \int_{V_j} \mathbf{B}^T \mathbf{D}_j \mathbf{B}\, dV_j \tag{4.6}$$

where $\mathbf{D}_j$ denotes the stress-strain relations matrix for the j-th layer of material (see Appendix C).

4.2 Boundary conditions in the delamination crack tip

To connect the elements *I* with elements *II* and *III*, modelling the delamination area and to satisfy continuity of the displacements the following conditions must be fulfilled (see Fig.4.2):

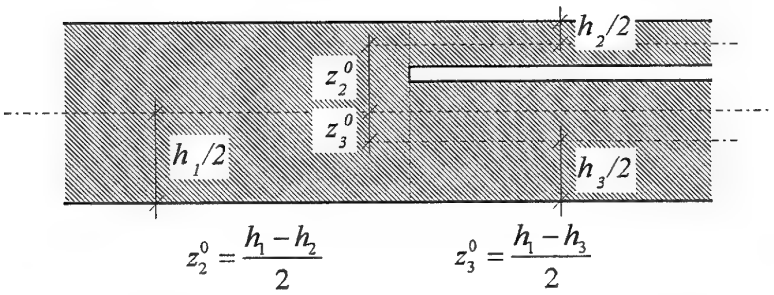

Fig.4.2. The cross-section of the plate in delamination crack tip.

$$\begin{cases} u_2^0 = u_1^0 - z_2^0 \cdot \phi_x, & u_3^0 = u_1^0 - z_3^0 \cdot \phi_x \\ v_2^0 = v_1^0 - z_2^0 \cdot \phi_y, & v_3^0 = v_1^0 - z_3^0 \cdot \phi_y \end{cases} \tag{4.7}$$

where z_2^0 and z_3^0 are the distances between neutral axes of elements *I-II* and *I-III*.

Applying relations (4.7) to (4.1), the displacement fields of elements *II* and *III* which model delamination region are obtained. Similarly, the inertia and stiffness matrices of these elements can be calculated.

5. Numerical calculations

5.1 Natural frequencies of cracked composite beam

The examples of numerical calculations showing the influence of the crack parameters (depth and position) and material parameters (volume of the fibre and the angle of the fibre) on the changes of the frequency of natural bending vibrations were carried on for the cantilever beam, which geometrical dimensions are shown in Fig. 5.1. It has been assumed that the beam is made of unidirectional composite material (graphite –fibre reinforced polyamide). Materials parameters of the components and relations to calculate the gross material coefficients for the analysed composite material are presented in Appendix A.

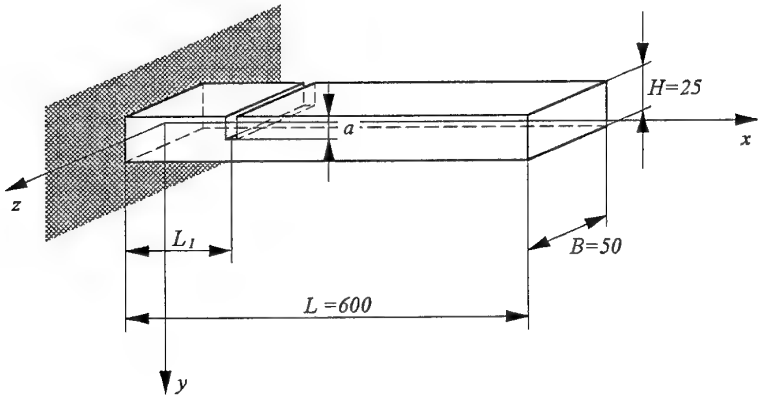

Fig. 5.1. Geometry of the cantilever composite beam with a transverse crack.

In all cases we assumed ten beam finite elements presented in the paper (including the element with the crack) to divide the analysed beam.

The numerical calculations were carried on a PC computer using a program written by the authors. For the standard eigenvalue problem the QL method was applied.

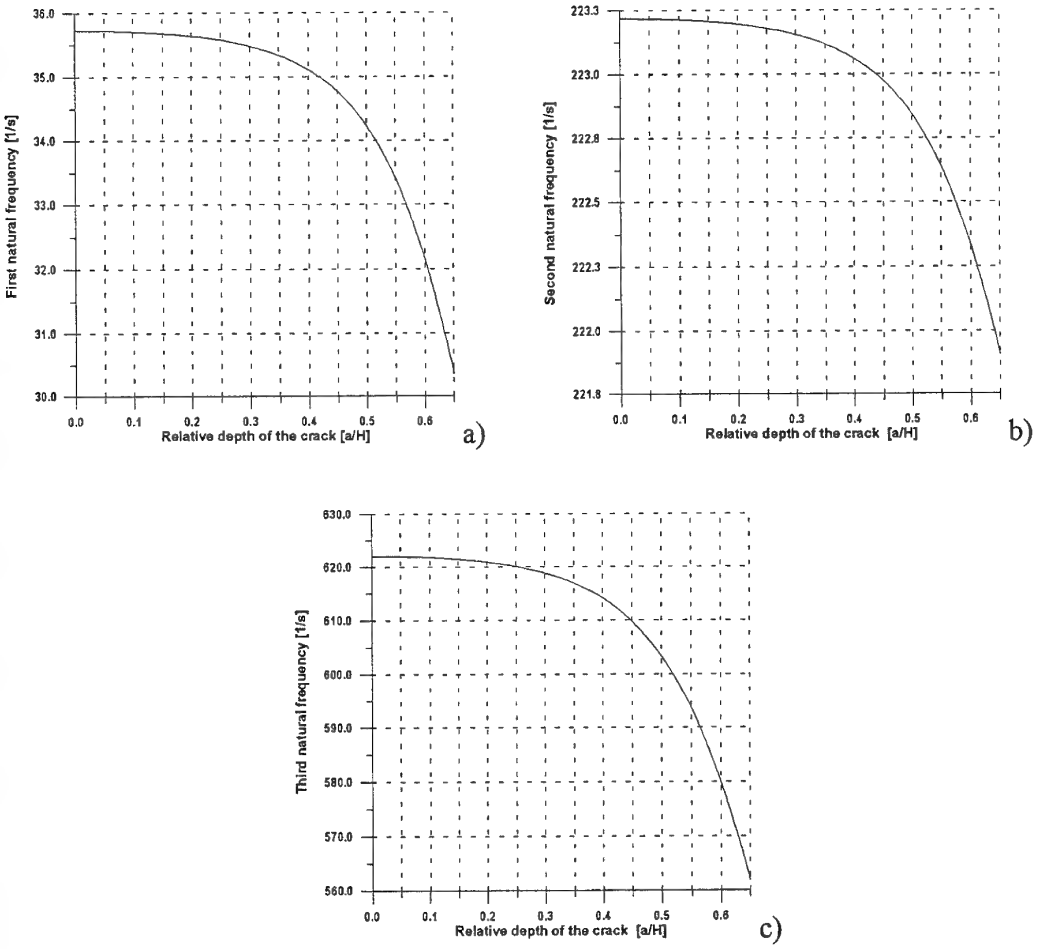

Fig.5.2 Influence of the crack depth on the first three natural frequencies of the cantilever composite beam a) first frequency, b) second frequency, c) third frequency.

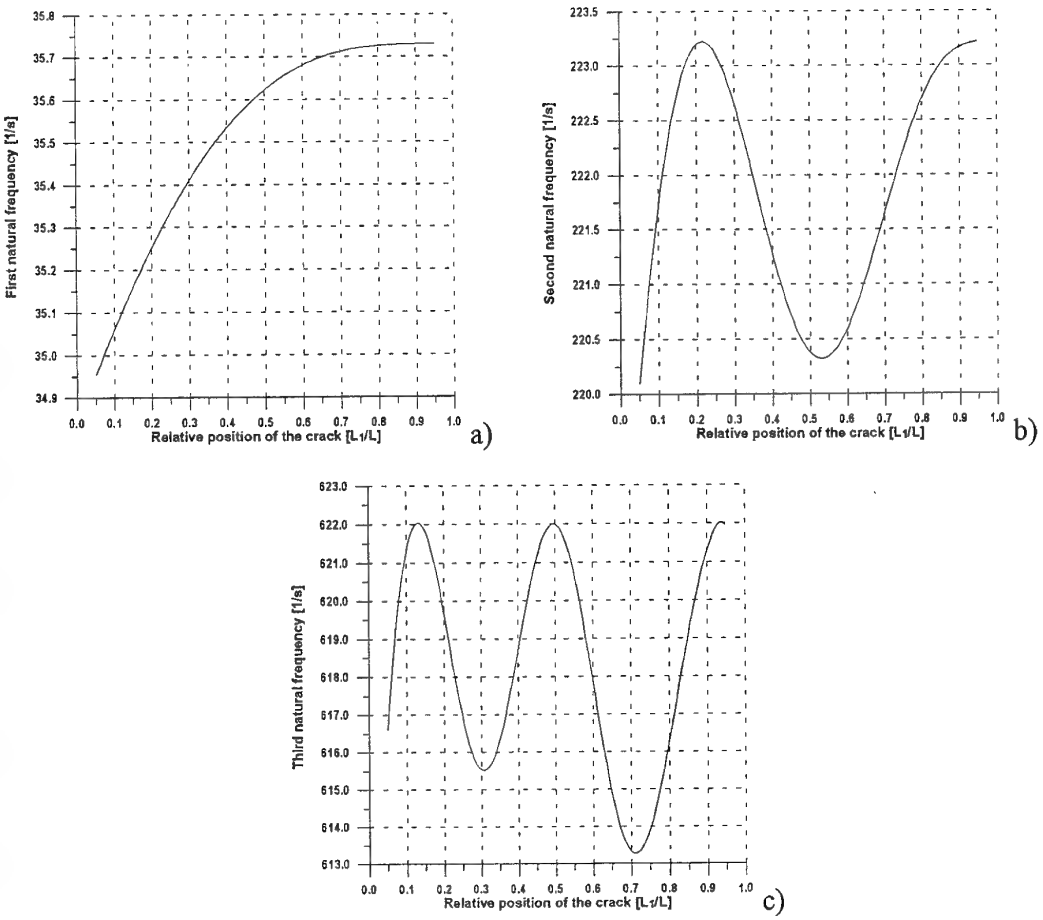

Fig.5.3 Influence of the crack location on the first three natural frequencies of the cantilever composite beam a) first frequency, b) second frequency, c) third frequency.

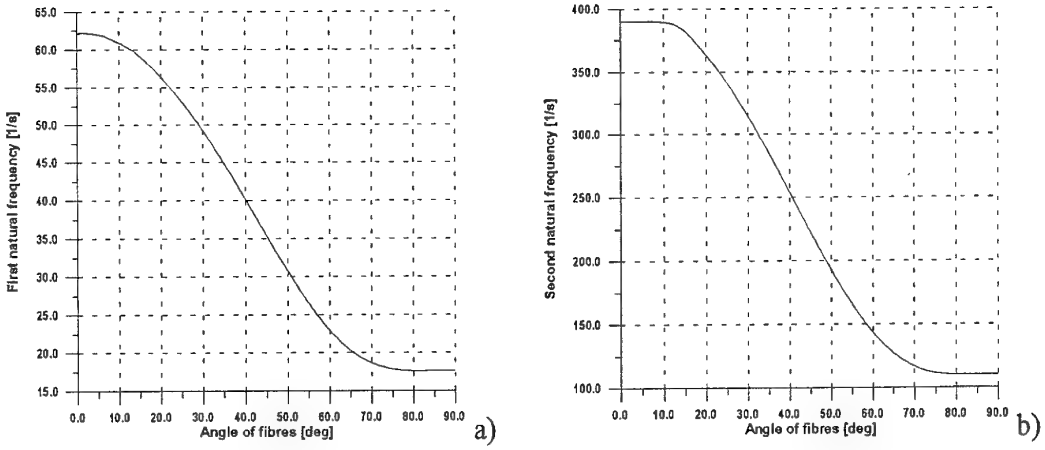

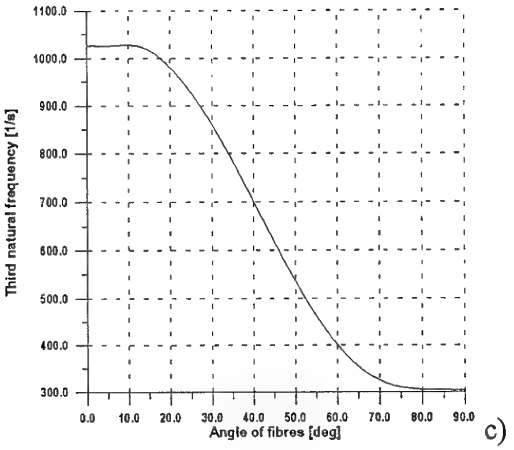

Fig. 5.4 Influence of the fibres angle on the first three natural frequencies of the cantilever composite beam a) first frequency, b) second frequency, c) third frequency.

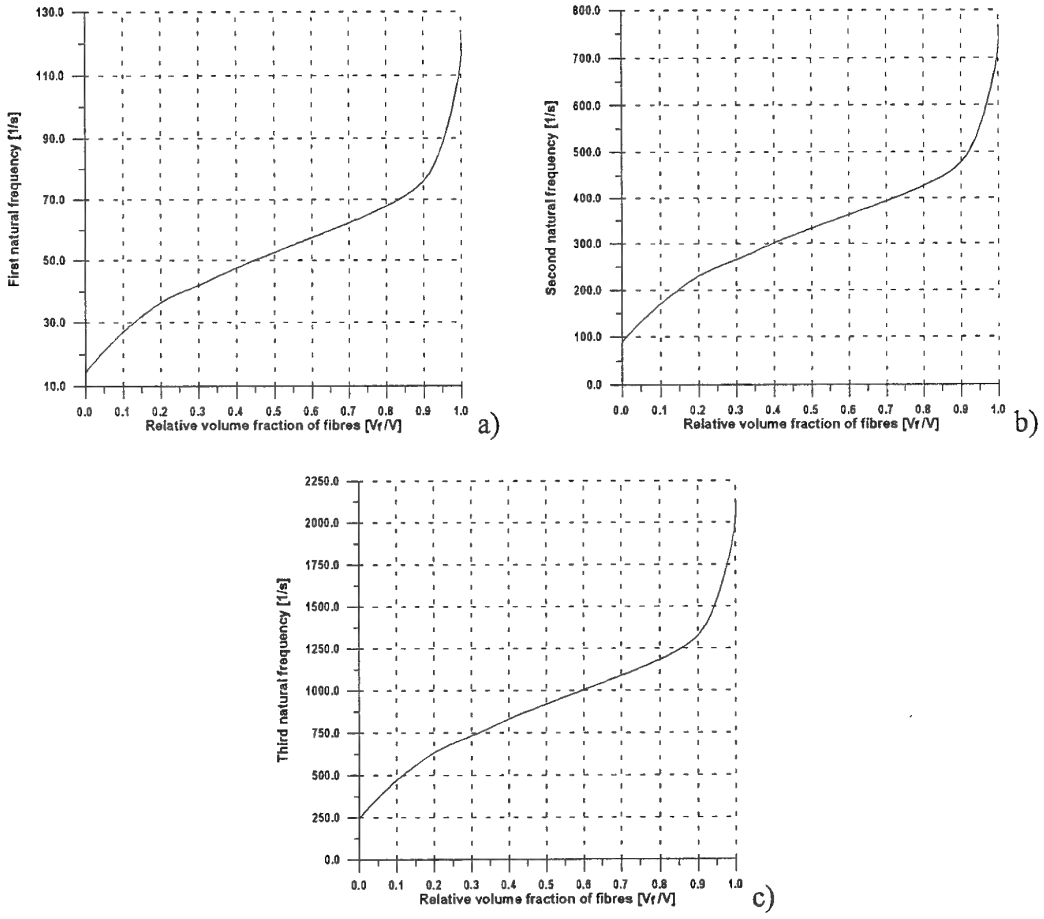

Fig.5.5 Influence of the fibres volume on the first three natural frequencies of the cantilever composite beam a) first frequency, b) second frequency, c) third frequency.

In Fig.5.2 and Fig.5.3 the results showing the influence of the depth and the position of the crack on the first three natural frequencies of the analysed beam are shown. Numerical calculations have been carried on assuming the overall volume of fibres of 20% and the angle of the fibre 45 degrees (measured between the geometric axis of the beam and the material principal axes).

From the Fig.5.2 and 5.3 it is clear, that the increase of the depth of the crack causes in each case decrease of the each calculated natural bending frequency of the analysed beam. The influence of the position of the crack on the changes of the i–th natural bending frequency of the analysed beam is more complicated and should be considered together with the character of the vibrations corresponding to that frequency. It shows, that the decrease of the considered natural frequency is most substantial when the crack is placed in the node and least substantial when the crack is placed in loop of vibrations. This can be explained by the fact that in the case of vibrations of the cantilever beam maximal bending moment appear in the nodes, while in the loops of vibrations bending moment is assumed zero. The decrease of stiffness in the crack corresponds (through the values of the stress) to the value of the bending moment. Hence, the highest decrease in the stiffness caused by the crack (and also the highest decrease of the natural bending frequency of the beam) of the same depth will occur always in the places where the bending moment is highest.

Fig.5.4 and Fig.5.5 show the influence of the material parameters (described by the angle of the fibres and relative volume of the fibres) on the changes of first three natural bending frequencies of the analysed beam. For calculations, we assumed non–changing position of the crack ($L_1/L = 0.25$) and constant value of its depth, namely 35% of the height of the beam.

Two conclusions could be obtained from Fig.5.4 and Fig.5.5. Firstly, with the increase of the angle of the fibre all natural bending frequencies of the beam increase with respect to the values of the natural bending frequencies of the beam without the crack. For all angles greater than 60 degrees, the decrease in the natural frequency caused by the crack

is almost unnoticeable. This conclusion does not concern the case of isotropic material, where the relative volume of the fibre equals 1 or 0.

Secondly, as a result of the numerical calculations it has been shown, that the decrease of the natural bending frequency of the beam caused by the crack strongly depends on the volume of the fibre. These facts could be explained by noticing the changes in factors D_1, D_2 in the function of the angle and relative volume of the fibre.

5.2 Natural frequencies of delaminated beam

The formulation of the elements and the method of modelling of the delaminated region of the beam have been evaluated by performing several example calculations.

Numerical calculations have been made for the cantilever beam of the following dimensions: length 600 mm, height 25 mm and width 50 mm. The beam was made of graphite-polyamide composite. It was assumed that all layers of the beam have the same mechanical properties, i.e., the volume fraction of fibers and the angle of fibers in each layer are identical. The mechanical properties of the applied material are given in Appendix A.

The first example illustrates the influence of the delamination position along the beam height upon the changes of the first bending natural frequency. The length of delamination was equal to 120 mm ($a/L = 0.2$) and the center of delamination was located 300 mm from the free end of the beam ($L_1/L = 0.5$). The angle of fibers (measured from x-axis of the beam) was 45 degrees., whereas the volume fraction of fibers was equal to 20% the volume of the beam. In this case the beam was discretized by 12 finite elements (4 elements in 2 layers around the region of delamination and 8 elements outside the delaminated region). The results of numerical calculations are given in Fig5.6. It is clearly shown that the largest drop in the first natural frequency is observed when the delamination is located along the neutral axis of the beam. When the delamination is located near the upper or the lower surface of the beam the changes in the first natural frequency can be neglected.

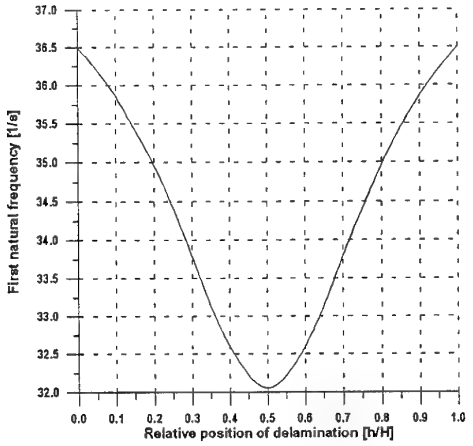

Fig.5.6. Influence of the delamination position (along the beam height) on the first natural frequency of the cantilever composite beam.

In the next example the influence of the length of the delamination upon the drop in bending natural frequencies of the analysed beam was observed. It was assumed that the delamination growth from the free end of the beam. The other parameters were the same as in the first example. The results of numerical calculations are presented in Fig.5.7. It is noted that when the length of the delamination increases the values of natural frequencies are greatly reduced. The intensity of these changes also depends on the number of natural frequencies (i.e., the mode shape and the location of delamination along the beam).

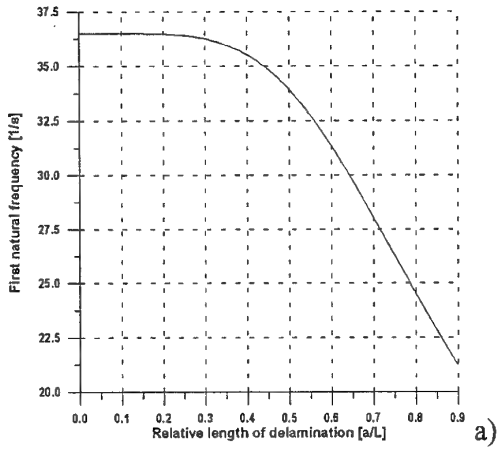

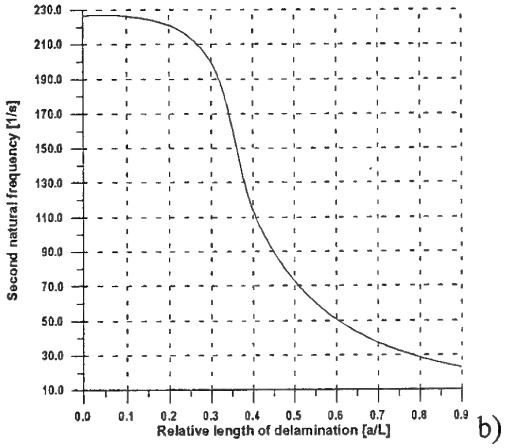

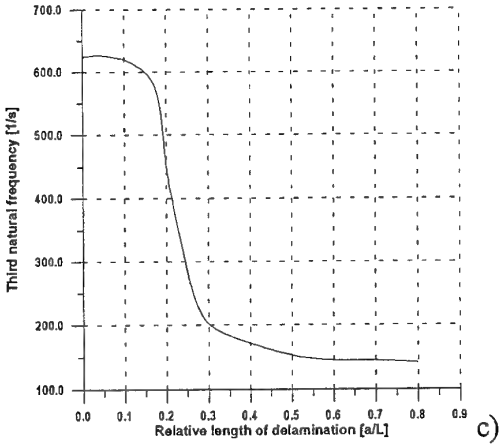

Fig.5.7 Influence of the delamination length on the first three natural frequencies of the cantilever composite beam a) first frequency, b) second frequency, c) third frequency.

The third example shows the influence of the location of delamination along the beam on the drop in bending natural frequencies. As in the first and second examples the beam was made of polyamide-graphite composite material. The delamination was located along the neutral axis of the beam. The length of delamination was equal to 37.5 mm $(a/L = 0.0625)$. Fig.5.8 illustrates the changes of analysed frequencies for different locations of the delamination. It is clearly shown that the changes in natural frequencies strongly depend on the location of delamination. For the analysed beam the largest drop in natural frequency is observed when the center of the delamination is located at the node of mode shape associated with this frequency.

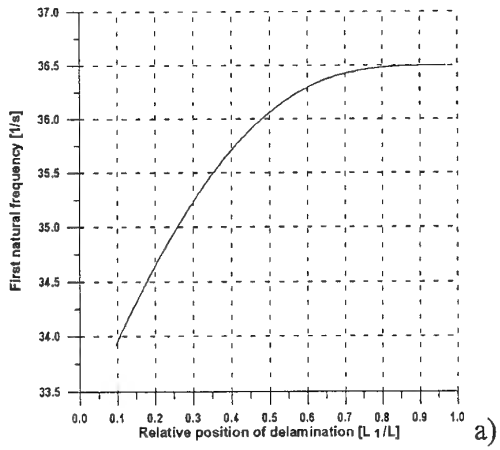

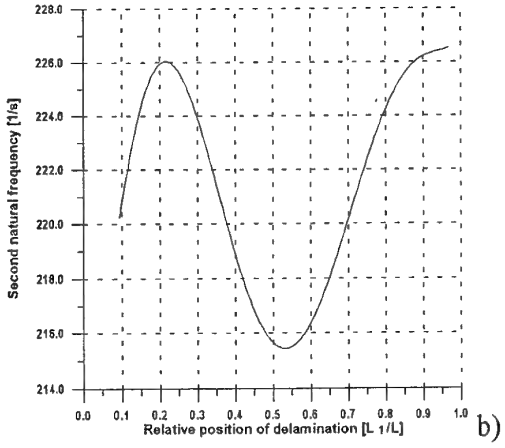

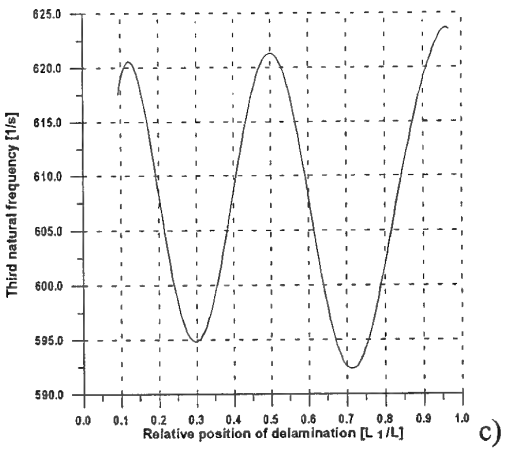

Fig.5.8 Influence of the delamination location on the first three natural frequencies of the cantilever composite beam a) first frequency, b) second frequency, c) third frequency.

5.3 Natural frequencies of delaminated plate

Numerical calculations for the cantilever composite plate have been carried out for the following plate dimensions: length 240 mm, width 120 mm and height 6 mm. The plate consisted six layers of materials with changing angle of fibres (+45 degrees in 1, 3, 5 layers and -45 degrees in 2, 4, 6). Each layer of the plate was made of graphite-polyamide composite. It was assumed that all mechanical properties except the angle of fibers are the same in each layer. The mechanical properties of the applied material are given in Appendix A.

The first example illustrates the influence of the delamination position along the plate height on the changes of the first bending natural frequency. The length of delamination was equal to 30 mm ($a/L = 0.125$) and the center of delamination was located 105 mm from the free end of the beam ($L_1/L = 0.4375$). The volume fraction of fibers was equal to 20% the volume of the plate. In this case the plate was discretized by 54 finite elements (42 elements in 2 layers around the region of delamination and 12 elements outside the delaminated region). The results of numerical calculations are given in Fig.5.9. It is clearly shown that the largest drop in the first natural frequency is

observed when the delamination is located along the neutral plane of the plate. When the delamination is located near the upper or the lower surface of the plate the changes in the first natural frequency can be neglected.

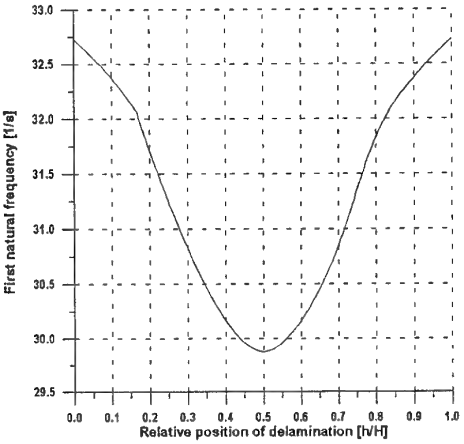

Fig.5.9 Influence of the delamination position (along the plate height) on the first natural frequency of the cantilever composite plate.

In the next example the influence of the length of the delamination upon the drop in bending natural frequencies of the analysed plate was observed. It was assumed that the delamination growth from the free end of the plate. The other parameters were the same as in the first example. The results of numerical calculations are presented in Fig.5.10. It is noted that when the length of the delamination increases the values of natural frequencies are greatly reduced. The intensity of these changes also depends on the number of natural frequencies (i.e., the mode shape and the location of delamination along the plate).

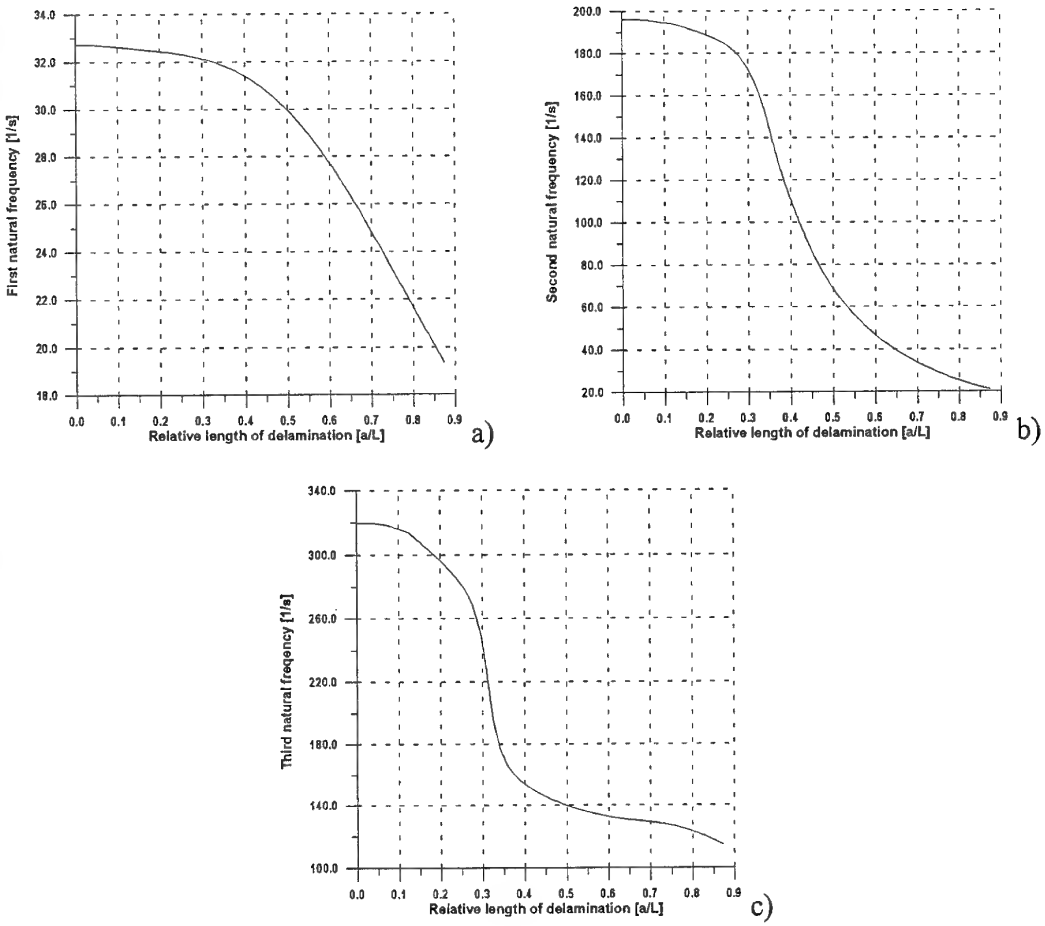

Fig.5.10 Influence of the delamination length on the first three natural frequencies of the cantilever composite plate a) first frequency, b) second frequency, c) third frequency.

The third example shows the influence of the location of delamination along the plate on the drop in bending natural frequencies. As in the first and second examples the plate was made of polyamide-graphite composite material. The delamination was located along the neutral plane of the plate. The length of delamination was equal to 30 mm $(a/L = 0.125)$. Fig.5.11 illustrates the changes of analysed frequencies for different locations of the delamination. It is clearly shown that the changes in natural frequencies strongly depend on the location of delamination. For the analysed plate the largest drop in natural frequency is observed when the center of the delamination is located at the node of mode shape associated with this frequency.

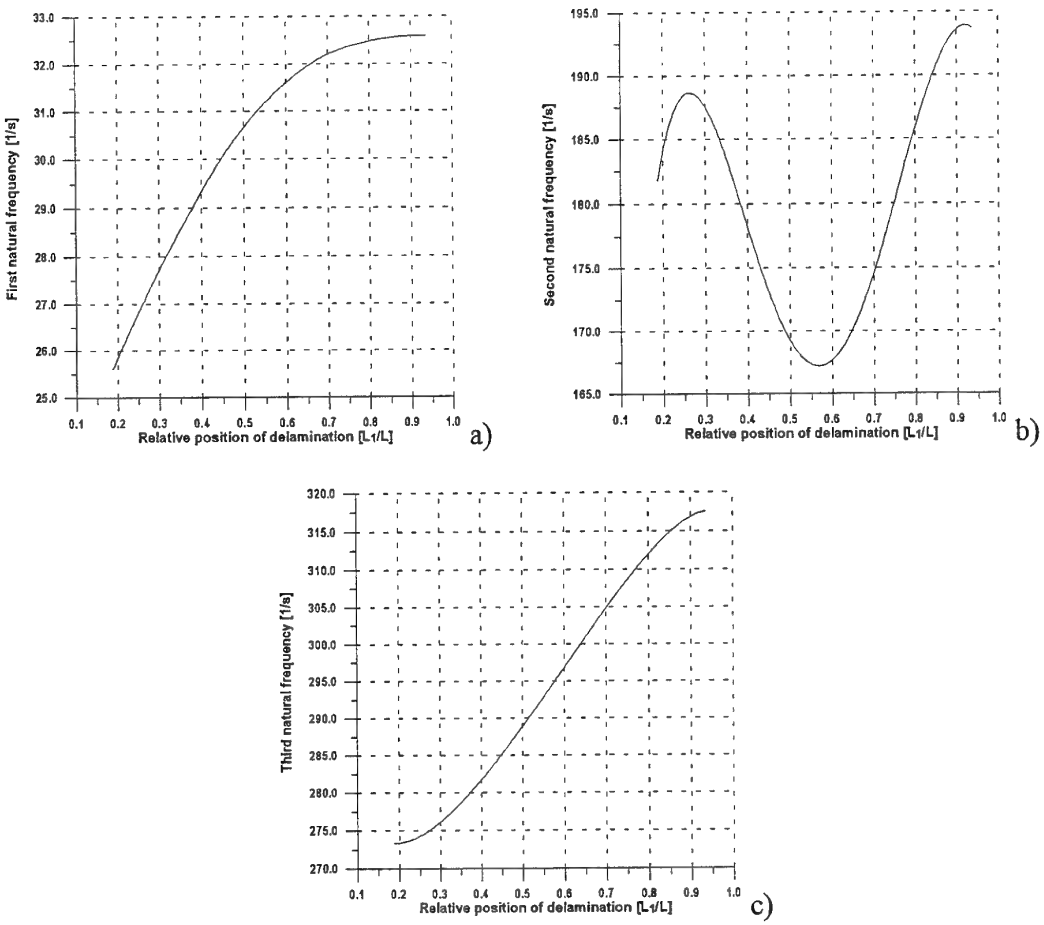

Fig.5.11 Influence of the delamination location on the first three natural frequencies of the cantilever composite plate a) first frequency, b) second frequency, c) third frequency.

5. Conclusions

As a result of this work models of the finite beam and plate elements have been elaborated, to enable the analysis of the influence of the fatigue cracks and delaminations on the dynamic characteristics of the constructions made of unidirectional composite materials. The method of modelling the crack or delamination presented in the paper enables an easy modification of the elaborated elements according to its specific damage (oblique crack, two–side crack, inside crack, multiple delaminations etc.).

The results of numerical calculations obtained from the crack model are in consistence with the known influence of the position and depth of the crack on the decrease of the natural bending frequencies of the cantilever beam. Simultaneously, a strong influence of the material parameters on these changes has been observed, which does not exist in the case of isotropic materials. The results above are also backed theoretically, but to justify them it is necessary to carry out the experimental research as well. A preparations to do this has already been made.

The method of modelling the delamination in composite beams and plates is versatile and allows analysis of the influence of multiple delaminations on natural frequencies of beams and plates with various boundary conditions. Using the elaborated models the effects of location and size of delamination on bending natural frequencies of composite beams and plates were studied.

Based on the numerical results, the following conclusions are drawn:

1) The delamination in cantilever composite beams and plates causes, as expected, reduction in bending natural frequencies.
2) The changes in natural frequencies are a function of the location and length of the delamination.
3) When the center of delamination is located at a point where the bending moment has the maximum value (for analysed mode shape) the reduction in the bending natural frequency associated with this mode is largest.
4) The largest drop in the bending natural frequencies is observed when the delamination is located along the neutral axis.
5) When the length of the delamination increases the drop in natural frequencies also increases.

6. Bibliography

[1] Dimarogonas A.D., Massouros G., "Torsional vibration of a shaft with circumferential crack". Engineering Fracture Mechanics. 15, 439-444, (1980).

[2] Gudmundson P., "The dynamic behavior of slender structures with cross-sectional cracks". Journal of Mechanical Physics Solids. 31, 329-345, (1983).

[3] Papadopoulos C.A., Dimarogonas A.D., "Coupling of bending and torsional vibration of a cracked Timoshenko shaft", Ingenieur Archiv, 57, 257-266, (1987).

[4] Shen M.H.H., Pierre C., "Natural modes of Bernoulli-Euler beams with a single edge cracks". Journal of Sound and Vibration. 138, 115-134, (1990).

[5] Chondros T.G., Dimarogonas A.D., "Identification of cracks in welded joints of complex structures". Journal of Sound and Vibration. 69, 531-538, (1981).

[6] Bently D.E., Muszyńska A., "Early detection of shaft cracks on fluid-handling machines". Proceedings of the International Symposium on Fluid Machinery Troubleshooting, 53-58, Anaheim, (1986).

[7] Ju F.D., Mimovich M.E., "Experimental diagnosis of fracture damage in structures by the modal frequency method". ASME Journal of Vibration, Acoustics, Stress, and Reliability in Design. 110, 456-463, (1988).

[8] Akgun M.A., "Damage diagnosis in frame structures with a dynamic response method". Journal of Mechanical Structures and Machines. 18, 175-196, (1990).

[9] Wauer, "Dynamics of cracked rotors. A Literature Survey". Journal of Applied Mechanics Review 17, 1–7 (1991).

[10] Adams R.D., Cawley P., Pye C.J., Stone J., "A vibration testing for non-destructively assessing the integrity of a structures". Journal of Mechanical Engineering Sciences, 20, 93-100, (1978).

[11] Cawley P., Adams R.D., "A vibration technique for non-destructive testing of fiber composite structures". Journal of Composite Materials, 13, 161-175, (1979).

[12] Nikpour K., Dimarogonas A.D., "Local compliance of composite cracked bodies". Journal of Composite Science and Technology, 32, 209-223, (1988).

[13] Nikpour K., "Buckling of cracked composite columns". Journal of Solids Structures 26, 1371–1386 (1990).

[14] Manivasagam S., Chandrasekaran K., "Characterisation of damage progression in layered composites". Journal of Sound and Vibration 152, 177–179 (1992).

[15] Chai, H., Babcock, C.D. and Knauss, W.G., "One dimensional modeling of failure in laminated plates by delamination buckling", International Journal of Solids and Structures, 17, 1069-1083, (1981).

[16] Bottega, W.J. and Maewal, A., "Delamination buckling and growth in laminates", Journal of Applied Mechanics, 50, 184-189, (1983).

[17] Whitcomb, J.D., "Parametric analytical study of instability related delamination growth", Composites Science and Technology, 25, 19-46, (1986).

[18] Yin, W.L., Sallam, S.N. and Simitses, G.J., "Ultimate axial load capacity of a delaminated beam-plate", AIAA Journal, 24,123-128, (1986).

[19] Chen, H.P., "Shear deformation theory for compressive delamination buckling and growth", AIAA Journal, 29, 813-819, (1991).

[20] Ramkumar, R.L., Kulkarni, S.V. and Pipes, R.B., "Free vibration frequencies of a delaminated beam", 34th Annual Technical Conference Proceedings: Reinforced Composites Institute, Society of Plastics Industry Inc., Section 22-E, pp.1-5, (1979).

[21] Wang, J.T.S., Liu, Y.Y. and Gibby, J.A., "Vibration of split beams", Journal of Sound and Vibration, 84, 491-502, (1982).

[22] Shen M.H.H., Grady J.E., "Free vibrations of delaminated beams". AIAA Journal. 30, 1361-1370, (1992).

[23] Yin W.L., Jane K.C., "Vibration of a delaminated beam-plate relative to buckled states". Journal of Sound and Vibration. 156, 125-140, (1992).

[24] Oral S., "A shear flexible finite element for nonuniform laminated composite beams". Computer and Structures. 38, 356-360, (1991).

[25] Tessler, S.B. Dong, "On a hierarchy of conforming Timoshenko beam elements". Computer and Structures 38, 334–344, (1991).

[26] Bao, S. Ho, Z. Suo, B. Fan, "The role of material orthotropy in fracture specimens for composites". Journal of Solid Structures 29, 1105–1116, (1992).

Appendix A

The properties of the graphite–fibre reinforced polyamide composite analysed in the paper are assumed as follows [9]:

	matrix (polyamide)	fibre (graphite)
elastic modulus	$E_m = 2.756$ GPa	$E_f = 275.6$ GPa
Poisson's ratio	$\nu_m = 0.33$	$\nu_f = 0.2$
rigidity modulus	$G_m = 1.036$ GPa	$G_f = 114.8$ GPa
mass density	$\rho_m = 1600$ kg/m^3	$\rho_f = 1900$ kg/m^3

The material is assumed orthotropic with respect to its axes of symmetry which lie along and perpendicularly to the direction of the fibre. The gross mechanical properties of the composite are calculated using the following formulate:

$$\rho = \rho_f \upsilon + \rho_m (1-\upsilon)$$

$$E_{11} = E_f \upsilon + E_m (1-\upsilon)$$

$$E_{22} = E_m \left[\frac{E_f + E_m + (E_f - E_m)\upsilon}{E_f + E_m - (E_f - E_m)\upsilon} \right]$$

$$\nu_{12} = \nu_f \upsilon + \nu_m (1-\upsilon)$$

$$\nu_{23} = \nu_f \upsilon + \nu_m (1-\upsilon) \left[\frac{1 + \nu_m - \nu_{12} E_m / E_{11}}{1 + \nu_m^2 - \nu_m \nu_{12} E_m / E_{11}} \right]$$

$$G_{12} = G_m \left[\frac{G_f + G_m + (G_f - G_m)\upsilon}{G_f + G_m - (G_f - G_m)\upsilon} \right]$$

$$G_{23} = \frac{E_{22}}{2(1-\nu_{23})}$$

where υ denotes the volume fraction of the fibre. The principal axes 1 and 2 are in the plane of the composite specimen aligned along and perpendicularly to the fibre directions.

Appendix B

The complex constants s_1 and s_2 are the roots of the presented characteristic equation [12]:

$$\bar{b}_{11} s^4 - 2\bar{b}_{16} s^3 + (2\bar{b}_{12} + \bar{b}_{66}) s^2 - 2\bar{b}_{26} s + \bar{b}_{22} = 0$$

where constants $\bar{b}_{ij}$ are calculated from the following relations:

$$\bar{b}_{11} = b_{11}m^4 + 2(b_{12} + b_{66})m^2n^2 + b_{22}n^4$$
$$\bar{b}_{22} = b_{11}n^4 + 2(b_{12} + b_{66})m^2n^2 + b_{22}n^4$$
$$\bar{b}_{12} = (b_{11} + b_{22} - 2b_{66})m^2n^2 + b_{11}(m^4 + n^4)$$
$$\bar{b}_{16} = (b_{11} - b_{12} - b_{66})m^3n + (b_{12} - b_{22} + b_{66})n^3m$$
$$\bar{b}_{26} = (b_{11} - b_{12} - b_{66})n^3m + (b_{12} - b_{22} + b_{66})m^3n$$
$$\bar{b}_{66} = 2(b_{11} - 2b_{12} + b_{22} - b_{66})m^2n^2 + b_{66}(m^4 + n^4)$$

where m= cos(α), n= sin(α), (α denotes the angle between the fibre direction and axis of the beam perpendicular to the crack–see Fig.2.1). The terms b_{ij} correspond to the situation when the geometric axes of the beam coincide with the material principal axes. These are related to the mechanical constants of the material by:

$$b_{11} = \frac{1}{E_{11}}\left(1 - \nu_{12}^2 \frac{E_{22}}{E_{11}}\right)$$
$$b_{22} = \frac{1}{E_{22}}(1 - \nu_{23}^2)$$
$$b_{12} = \frac{-\nu_{12}}{E_{22}}(1 + \nu_{23})$$
$$b_{66} = \frac{1}{G_{12}}$$

Roots of the characteristic equation are either complex or pure imaginary and can not be real. Thus, the four roots separate into two sets of distinct complex conjugates. The parameters s_1 and s_2 correspond to those with positive imaginary parts.

Appendix C

In the case of analysed beam elements, the stress–strain relations matrix posses the form:

$$\mathbf{D} = \begin{bmatrix} \bar{S}_{11} & \bar{S}_{16} \\ \bar{S}_{16} & \bar{S}_{66} \end{bmatrix}$$

while for the plate element, the stress-strain relation matrix can be written as:

$$\mathbf{D} = \begin{bmatrix} \overline{S}_{11} & \overline{S}_{12} & \overline{S}_{16} & & \\ \overline{S}_{12} & \overline{S}_{22} & \overline{S}_{26} & & \\ \overline{S}_{16} & \overline{S}_{26} & \overline{S}_{66} & & \\ & & & \overline{S}_{44} & \overline{S}_{45} \\ & & & \overline{S}_{45} & \overline{S}_{55} \end{bmatrix}$$

Elements of matrix **D** can be calculated from following relations:

$$\begin{aligned}
\overline{S}_{11} &= S_{11}m^4 + S_{22}n^4 + 2(S_{12} + S_{66})m^2n^2 \\
\overline{S}_{12} &= (S_{11} + S_{22} - 2S_{66})m^2n^2 + S_{12}(m^4 + n^4) \\
\overline{S}_{22} &= S_{11}n^4 + S_{22}m^4 + 2(S_{12} + S_{66})m^2n^2 \\
\overline{S}_{16} &= (S_{11} - S_{12} - S_{66})m^3n + (S_{12} - S_{22} + S_{66})n^3m \\
S_{26} &= (S_{11} - S_{12} - S_{66})n^3m + (S_{12} - S_{22} + S_{66})m^3n \\
\overline{S}_{66} &= 2(S_{11} + S_{22} - 2S_{12} - S_{66})m^2n^2 + S_{66}(m^4 + n^4) \\
\overline{S}_{44} &= S_{44}m^2 + S_{55}n^2 \\
\overline{S}_{45} &= (S_{55} - S_{44})mn \\
\overline{S}_{44} &= S_{44}n^2 + S_{55}m^2
\end{aligned}$$

where m= cos(α), n= sin(α), (α denotes the angle between the fibre direction and neutral axis).

The terms S_{ij} corresponding with the material principal axes are determined in all cases by following formulas:

$$S_{11} = \frac{E_{11}}{1 - \nu_{12}\nu_{21}}$$

$$S_{22} = \frac{E_{22}}{1 - \nu_{12}\nu_{21}}$$

$$S_{12} = \frac{-\nu_{12}E_{11}}{1 - \nu_{12}\nu_{21}}$$

$$S_{66} = G_{12}, \quad S_{44} = G_{23}, \quad S_{55} = G_{13}$$

List of all participating scientific personnel

1. Wiesław M. Ostachowicz; Ph.D., Dr.Sc., Full Professor
2. Marek Krawczuk; Ph.D.
3. Arkadiusz Żak; M.Sc.

M. Krawczuk expects to receive his Dr.Sc. this autumn based, in part, upon work done in this project.

A. Żak expects to receive his Ph.D. next autumn based, in part, upon work done in this project. A copy of this thesis will be submitted when it becomes available.

List of all publications and technical reports published

1) Ostachowicz W., Krawczuk M.: *Dynamic analysis of delaminated composite beam.* Machine Vibration (Springer-Verlag), No.3, pp.107-116, **1994.**
2) Krawczuk M., Ostachowicz W., Żak A.: *Analysis of natural frequencies of delaminated composite beams based on finite element method.* An International Journal Structural Engineering and Mechanics (paper accepted for publication - 16 May **1995**).
3) Krawczuk M., Ostachowicz W., Żak A.: *Modal analysis of cracked unidirectional composite beam.* An International Journal Composites Engineering (paper submitted for publication - 3 March **1995**)
4) Ostachowicz W., Krawczuk M., Żak A.: *The analysis of the influence of the fatigue crack on the changes of the natural frequencies for the unidirectional composite cantilever beam.* [Proceedings] II International Conference on Composites Engineering, New Orleans, LA, 20-24 August 1995.
5) Krawczuk M., Ostachowicz W., Żak A.: *Natural frequencies of delaminated composite beam.* Proceedings: XII Polish Conference on Computer Methods in Mechanics, Warsaw-Zegrze, Poland, 9-13 May 1995, pp.171-172.
6) Żak A., Krawczuk M., Ostachowicz W.: *Analiza wpływu pęknięcia zmęczeniowego na zmiany częstości drgań własnych belki wspornikowej wykonanej z jednokierunkowego materiału kompozytowego (The analysis of the influence of the fatigue crack on the changes of the natural frequencies for unidirectional composite cantilever beam).* Reports of The Institute of Fluid Flow Machinery, No.366/94.
7) Krawczuk M., Żak A., Ostachowicz W.: *Kompozytowy płytowy element skończony z delaminacją. Koncepcja ogólna oraz podstawowe związki. (The plate finite element with delamination).* Reports of The Institute of Fluid Flow Machinery, No.96/95.

8) Żak A., Krawczuk M., Ostachowicz W.,: *Analiza numeryczna belek i płyt kompozytowych z delaminacją (Numerical analysis of delaminated composite beams and plates).* Reports of The Institute of Fluid Flow Machinery, No.171/95.